ELSEVIER

Journal of Organometallic Chemistry 530 (1997) 131–140

Journal of Organometallic Chemistry

Cone angle radial profiles

Jeremy M. Smith, B. Craig Taverner, Neil J. Coville *

Chemistry Department, University of the Witwatersrand, Private Bag 3, Wits 2050, Johannesburg, South Africa

Received 10 May 1996

Abstract

Various methodologies have been reported in the literature for the evaluation of the size of a ligand or organic functional group, with the Tolman cone angle methodology proving to be most popular in inorganic chemistry. A procedure to extend the Tolman concept to the measurement of a ligand size, as a profile over a radial distance from the metal (apex), has been developed. The representation of the Tolman cone angle as a function of distance from the metal is termed a cone angle radial profile (CARP). CARPs for PH_3, PMe_3, PEt_3 and PPh_3 have been determined and are described. CARPs for molecules containing the constrained phosphite ligands $P(OCH_2)_3CMe$, as determined in actual structures (Cambridge Structural Database), have also been evaluated and indicate the invariant shape of the ligand in the different metal environments. The influence of the choice of the H atom van der Waals radius in steric measurements is also discussed.

Keywords: Phosphines; Cone angles; Steric measurements; Group 15

1. Introduction

In attempting to rationalize reaction rates, chemical equilibria, crystallographic data, etc., chemists generally invoke the use of steric and electronic properties which are associated with either reactants or products. For example, in rationalizing a measurement, such as a reaction rate, a commonly used expression is

$$\text{measurement} = aS + bE$$

where a and b are constants and S and E refer to a steric and electronic property associated with one of the reagents [1]. Elaboration of this expression to give more complex expressions in which the S and E terms can be further subdivided is possible. For example the electronic term E can be divided into σ and π components [2]

$$bE = c\sigma + d\pi \quad (c \text{ and } d \text{ are constants})$$

There are a variety of procedures for measuring E and S. In inorganic chemistry, quantification of the steric component S can be achieved using cone angles θ [3], solid angles Ω [4], and repulsive energies E_R [5]. The above methods have associated advantages and disadvantages [3–5], and attempts to refine the methodologies for evaluating S are constantly being sought [6].

In this publication we wish to extend the use of the Tolman cone angle θ and propose a simple method for representing this extension.

In the original Tolman cone angle methodology, steric measurements of phosphine and phosphite ligands were achieved by placing the ligand P atom 2.28 Å from an apex, M (a metal atom), and enclosing the ligand in a cone generated from the apex (Fig. 1). For symmetrical ligands the cone angle was measured at the point which gave the largest θ on the ligand, and all cone angles were measured with a constant M–P bond distance to provide a comparative set of cone angle data. For unsymmetrical ligands the cone angle measurement is more complex [3] (see Appendix A).

This same procedure has been adopted for the cone angle measurements of amines [7], cyclopentadieny ligands [8], isonitriles [9], alkyl groups [10], etc.

In all the reports on cone angle discussions to date the cone angle has been measured at only one distance from the apex M (Fig. 1). Implicit in the measurement is the assumption that the ligand fully occupies the cone at the chosen distance. Modification to show the actual shape of the ligand within the cone has been achieved by means of ligand profiles, i.e. ligand angular profiles, which indicate the ligand shape in either Cartesian [11]

* Corresponding author. Fax: (+27) (011) 339-7967; e-mail: dept@aurum.chem.wits.ac.za.

0022-328X/97/$17.00 © 1997 Elsevier Science S.A. All rights reserved.
PII S0022-328X(96)06591-6

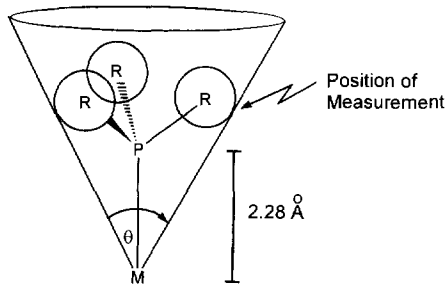

Fig. 1. Measurement of a Tolman cone angle θ [3].

or polar [12] coordinates. An example which indicates the ligand profile of a PR_3 ligand is shown in Fig. 2.

The issue of cone angle measurements at other positions along the length of a ligand, as measured from the metal, has not as yet been elaborated on in the literature. Herein we describe a general procedure for representing the change of cone angle along a metal–ligand vector. This representation will be referred to as a cone angle radial profile (CARP). The CARP could provide for an understanding of inter-ligand meshing, e.g. of two ligands attached to a common apex (a metal atom). It is to be noted that similar considerations have recently been given to the measurement of solid angle Ω radial profiles (SARPs) [13] and comparisons between the two studies will also be described.

2. Methods section

An algorithm to permit calculation of a cone angle of an intersecting sphere at any distance from an apex, similar to that for determination of solid angles, has been written (see Appendix A). The cone angle is thus determined from the cone produced by the intersection of atoms with a sphere of radius at which a calculation is being made (see Fig. 3).

Although this methodology is similar to that for

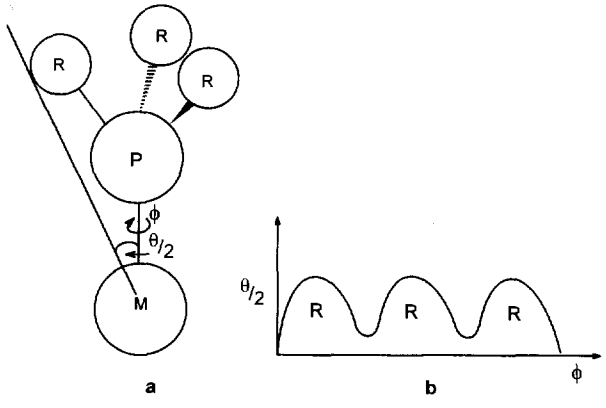

Fig. 2. Measurement of a Tolman ligand profile: (a) variation of $\theta/2$ as rotation occurs around the M–P axis; (b) variation of actual cone angle ($\theta/2$) as ϕ rotates through 360°.

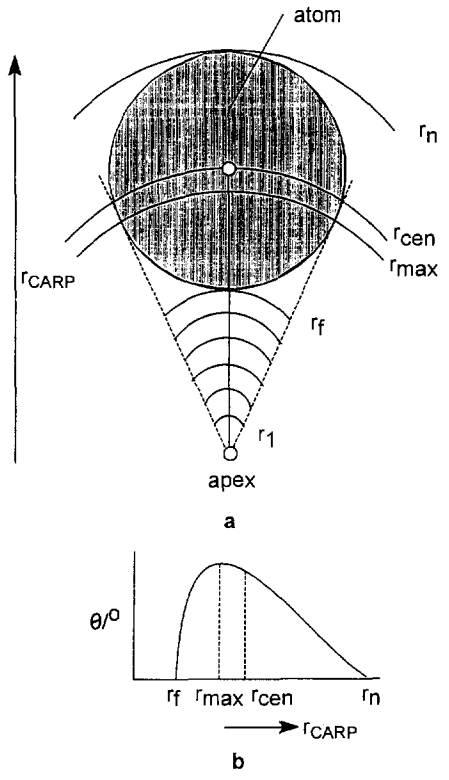

Fig. 3. (a) An atom (shaded) is placed a distance from r_{CARP} from an apex. Spheres or radius r to r_n are then constructed from the apex; r_f corresponds to the radius of a sphere which first intersects the atom and r_n the radius of a sphere touching the outermost point of the atom. (b) The variation of Ω with r_{CARP} as determined by using the solid angle algorithm.

determining a SARP, it will also be described here. In the procedure, a range of spheres of different radii radiating out from an apex yield a range of cone angles. Alternatively phrased, if a sphere of variable radius r is permitted to grow from the apex to beyond the atoms(s) under consideration then cone angles can be measured at each radius. Let us consider a single atom placed a distance d from an apex (e.g. a metal atom). A sphere is allowed to grow outwards from the apex with radius $r_1, r_2 \ldots r_n$ (Fig. 3). A sphere of radius r_f is the first radius to intersect the atom, and a sphere of radius r_n is the final radius to intersect the atom. As the radius r increases from r_f to r_{max} the cone angle will increase; thereafter it will decrease until, at r_n, $\theta = 0$. The variation of θ with distance as determined by the algorithm is shown graphically in Fig. 3(b). The variation of θ with r_{CARP} is called a CARP. The maximum cone angle θ_{max} is determined at r_{max}. A 3-D representation of the CARP may be obtained by plotting a circle with a cone angle of θ_{CARP} at each r_{CARP}.

All calculations for PH_3, PMe_3, PEt_3 and PPh_3 were performed on ligand conformations previously determined [5]. For $P(OCH_2CH_3)CCH_3$ the ligand conformations were obtained from both molecular mechanics calculations [5] and crystallographic data in the Cam-

bridge Structural Database (vers. 5.09). Unless otherwise indicated, the Bondi data set [14] was used for covalent and van der Waals radii.

3. Discussion

The approach to be used in the description of the change of cone angle of a ligand with distance from an apex (the CARP) will be to start with a simple system and then develop complexity into the system.

3.1. CARP of a spherical ligand

A radial plot of the cone angle of a sphere (e.g. Cl^-) of radius 0.5 Å, situated 2 Å from an apex (e.g. a metal atom), as a function of r_{CARP} is shown in Fig. 4(a), while Fig. 4(b) shows an equivalent 3-D representation of the CARP. Since cone angle and solid angle measurements are equivalent for the one sphere problem, and the issue relating to solid angle measurements has been dealt with in greater detail elsewhere [13], further comment on the shape of the CARP will not be made here.

The CARP varies with metal–sphere distance d_{M-S}, as shown in Fig. 5. In this figure a sphere S, of radius 0.5 Å, is moved from the apex M (up to a distance of 10 Å). The cone angle shows major changes when $d_{M-S} < 3$ Å, and the figure indicates that the ligand size, from the perspective of M, is a variable becoming, not unexpectedly, larger as d_{M-S} decreases.

3.2. CARP of more complex ligands

Extension of the ideas contained above to ligands comprising more than one atom can readily be achieved. Some simple examples to highlight the issues follow.

3.2.1. PH_3

The CARP determined using the Tolman approach for θ measurement is shown in Fig. 6(a). For the symmetrical ligand the Tolman cone angle listed in

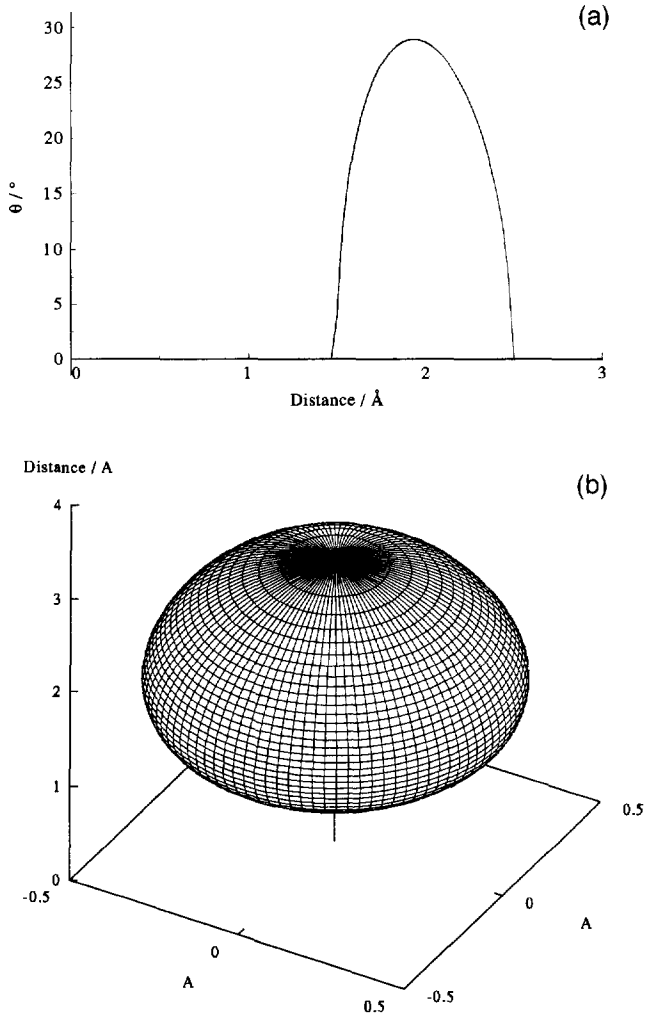

Fig. 4. (a) CARP of a sphere of radius 0.5 Å placed 2 Å from an apex. (b) 3-D CARP of a sphere of radius 0.5 Å placed 2 Å from an apex.

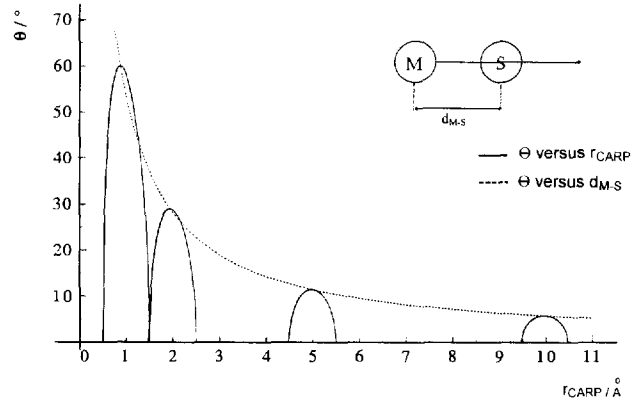

Fig. 5. Variation of the cone angle of a sphere(s) with distance from an apex (M). The CARPs are shown for a sphere of radius 0.5 Å as d_{M-S} is varied.

tables of cone angles corresponds to the cone angle of the ligands measured at r_{max} (e.g. PH_3; $\theta = 87°$ [3]). A 3-D representation of the CARP corresponding to Fig. 6(a) is shown in Fig. 6(b). Here the cone angle is shown as a function of distance from the metal (r_{CARP}) along the metal–P bond vector. The figure clearly indicates the variation of θ with r_{CARP}. It is also apparent that small variations in the d_{M-P} length will have little effect on the way in which this ligand will mesh with other ligands attached to the apex (the metal), as indicated by the flatness of the profile between 2.5 and 4.5 Å (Fig. 6(a)).

A 3-D representation of PH_3 based on the ligand angular profile approach [11,12] to θ measurement can also be determined (Fig. 6(c)). This figure more accurately reflects the shape of the ligand as a function of distance from the apex, and indicates how the changing ligand profile can also be represented graphically. Some 2-D slices of the profiles are also shown in the x–y plane in Fig. 6(c). The slices show how the cone angle varies with r_{CARP} and clearly reveal the non-spherical nature of the representation.

3.2.2. PMe_3

This ligand can also be classified as a 'simple' ligand, even though the maximum steric size is being measured at a position three atoms (P, C, H) removed from the apex (metal). Since the high symmetry of the ligand results in a restricted number of conformers, conformers do not significantly influence the steric size of this ligand. A CARP is shown in Fig. 7(a) and shows the variation of θ with r_{CARP} along the M–P bond vector. Again the small variation of θ between 3 and 4 Å from the apex is to be noted. It is also to be observed that the figure indicates three features. These correspond to the P atom, the two protons of each CH_3 group which are equidistant from P, and the third H atom of each group which lies away from the P atom.

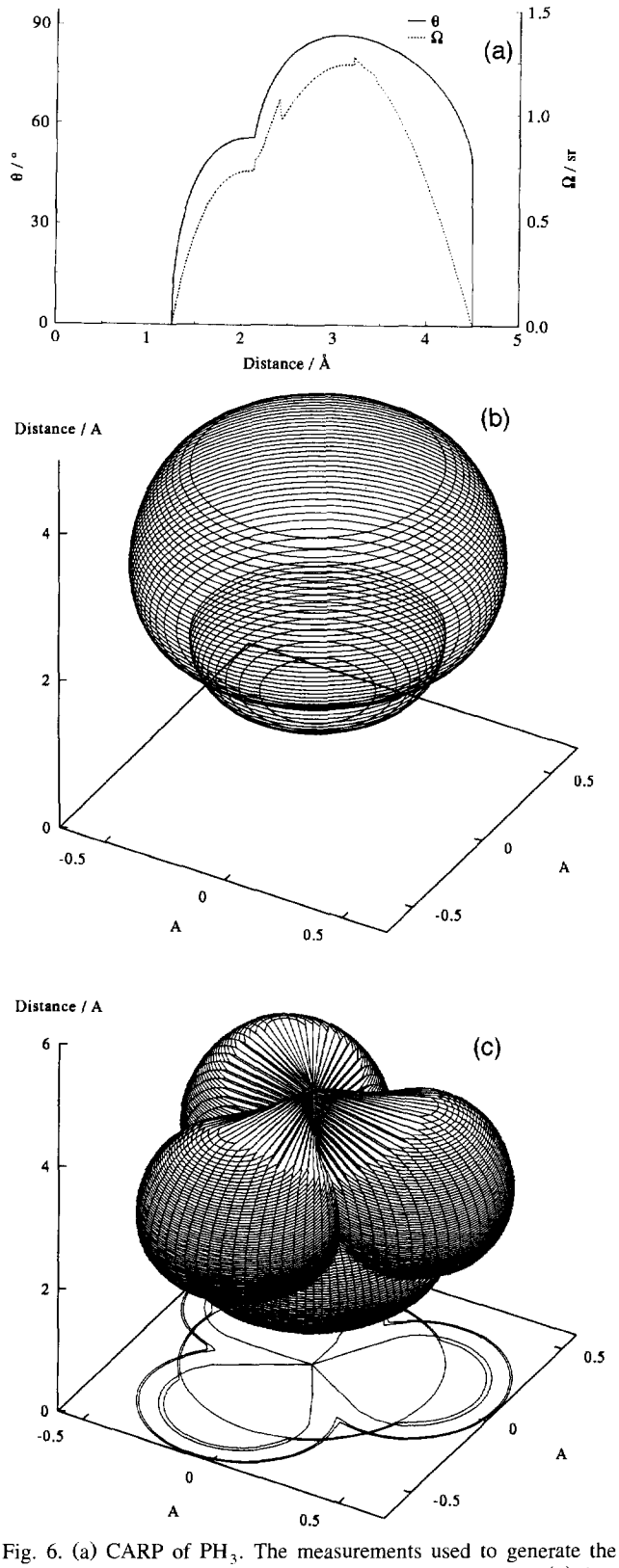

Fig. 6. (a) CARP of PH_3. The measurements used to generate the figure are based on the Tolman cone angle methodology. (b) 3-D representation of a CARP of PH_3. The measurements used to generate the figure are based on the Tolman cone angle methodology. (c) The variation of the PH_3 ligand profile (cone angle) with r_{CARP}.

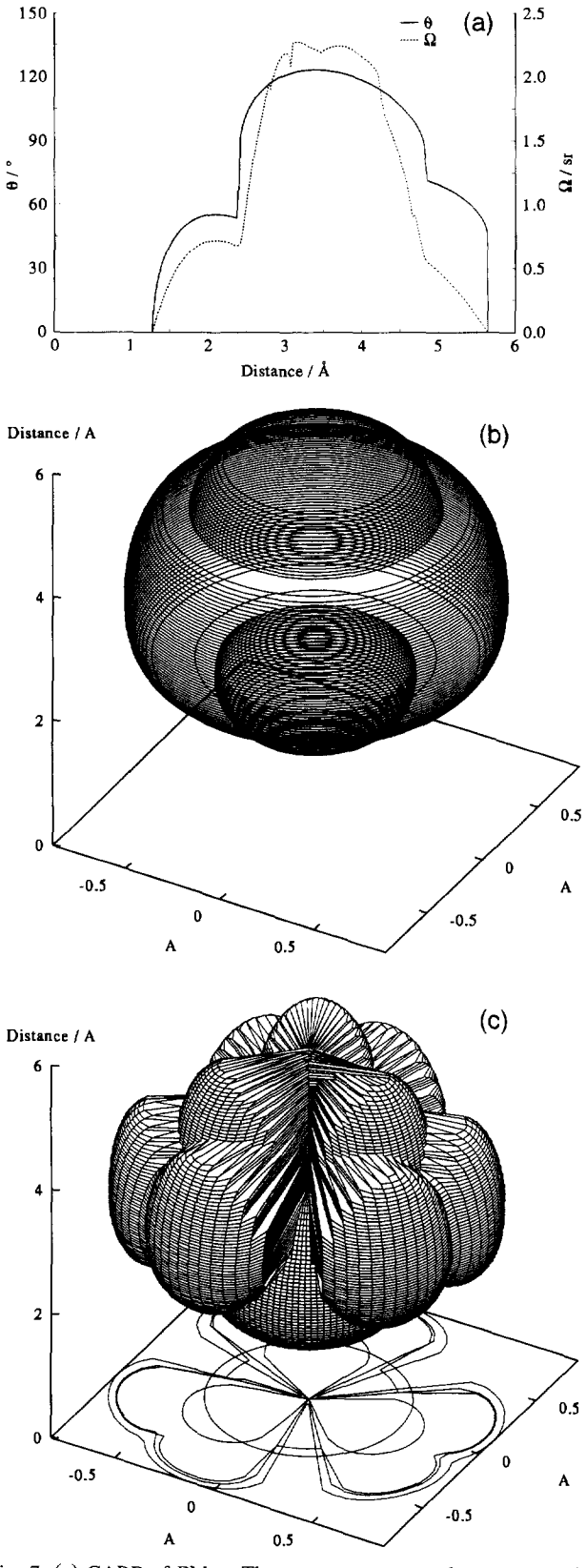

Fig. 7. (a) CARP of PMe_3. The measurements used to generate the figure are based on the Tolman cone angle methodology. (b) 3-D representation of a CARP of PMe_3. The measurements used to generate the figure are based on the Tolman cone angle methodology. (c) The variation of PMe_3 ligand profile (cone angle) with r_{CARP}.

The 3-D ligand profile representation of PMe_3 as a function of r_{CARP} is shown in Fig. 7(c) with some 2-D slices shown in the x–y plane. The more detailed description of the ligand size with r_{CARP} variation is apparent in these 2-D slices.

3.2.3. PEt_3

Since this ligand has 'floppy' organic groups, i.e. the CH_2CH_3 portion of the ligand can adopt a variety of conformations, some means to determine the lowest energy conformer is required. As in previous work, we have used the Brown-derived [5] conformer for our studies. The CARP for PEt_3 is shown in Fig. 8(a) and a representation of the CARP in 3-D is shown in Fig. 8(b). Fig. 8(a) and Fig. 8(b) show the shape of the ligand when the Tolman approach is used. The tabulated Tolman cone angle (for PEt_3; $\theta = 132°$ [3]) is smaller than the corresponding maximum value measured in Fig. 8(a). This relates to the choice of conformer; an issue dealt with by Stahl and Ernst [15], as well as the choice of the van der Waal radius of H (see below). Fig. 8(a) clearly reveals that the maximum value hardly varies between 2.5 and 3.5 Å.

Fig. 8(c) shows the ligand profile 3-D plot, which again more accurately reflects the complex shape of the PEt_3 ligand (2-D slices are shown in the x–y plane.)

3.2.4. PPh_3

The issues described in Sections 3.2.1, 3.2.2 and 3.2.3 are more clearly evidenced in the radial profiles for PPh_3 shown in Fig. 9(a) and Fig. 9(b). The conformer used in our study for PPh_3 was taken from the work of Brown and coworkers [5]. The CARP (Fig. 9(a)) and its 3-D representation, (Fig. 9(b)) for PPh_3 reveals the manner in which the cone angle of PPh_3 varies with r_{CARP} along the M–P axis. It is apparent from Fig. 9(b) that the meshing issue cannot be dealt with adequately if the Tolman cone angle is used to define size. Indeed Fig. 9(b) would suggest that between 3 and 7 Å very little meshing of PPh_3 with neighbouring ligands should be possible.

Fig. 9(c) shows a ligand profile 3-D plot of PPh_3; clearly the meshing issue can readily be predicted here. The less spherical a ligand the more the possibility for meshing with neighbouring ligands. What is also clear is that the 2-D ligand profiles shown in the x–y plane of Fig. 9(c) gives a representation which potentially can quantify any meshing issue. However, to date we have not been able to adequately draw this representation in a useful way.

3.3. Ligand–ligand overlap

It is clear from the above representation of ligand CARPs that a description of a ligand can be given by an angular cone angle analysis. Further, by comparing two

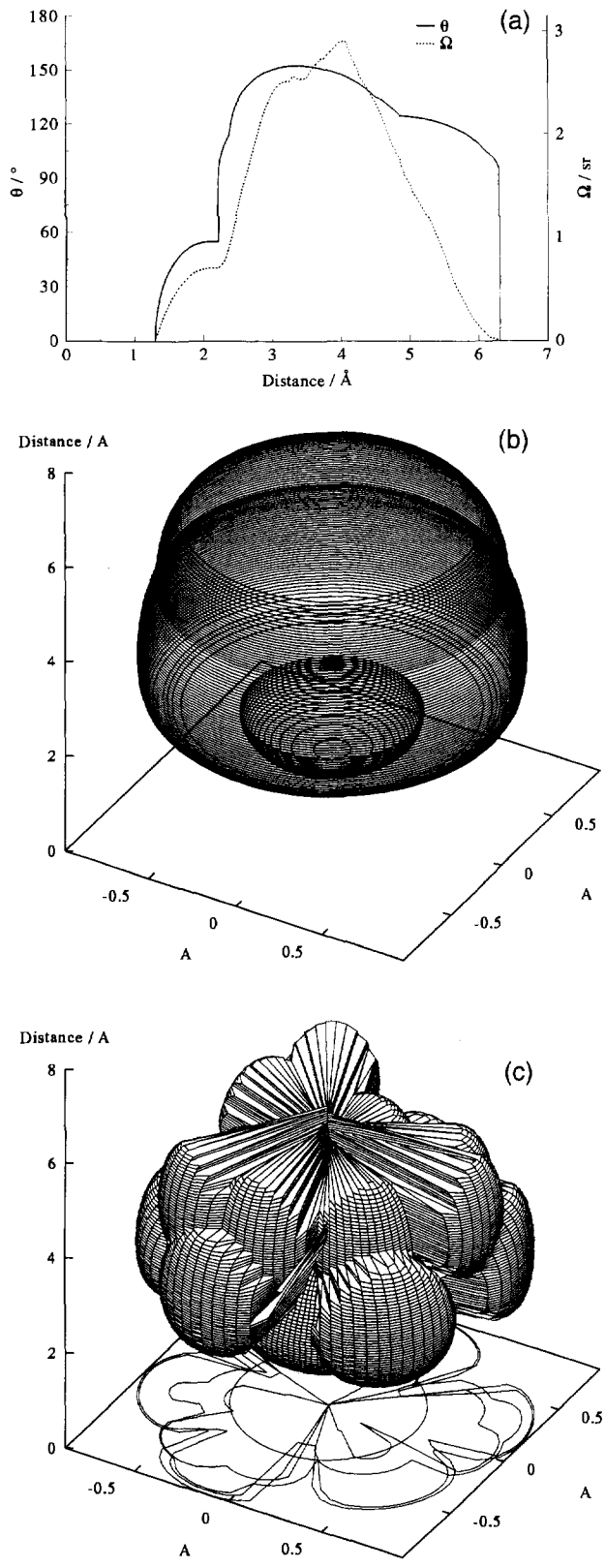

Fig. 8. (a) CARP for PEt_3. The measurements used to generate the figure are based on the Tolman cone angle methodology. (b) 3-D representation of a CARP for PEt_3. The measurements used to generate the figure are based on the Tolman cone angle methodology. (c) The variation of PEt_3 ligand profile (cone angle) with r_{CARP}.

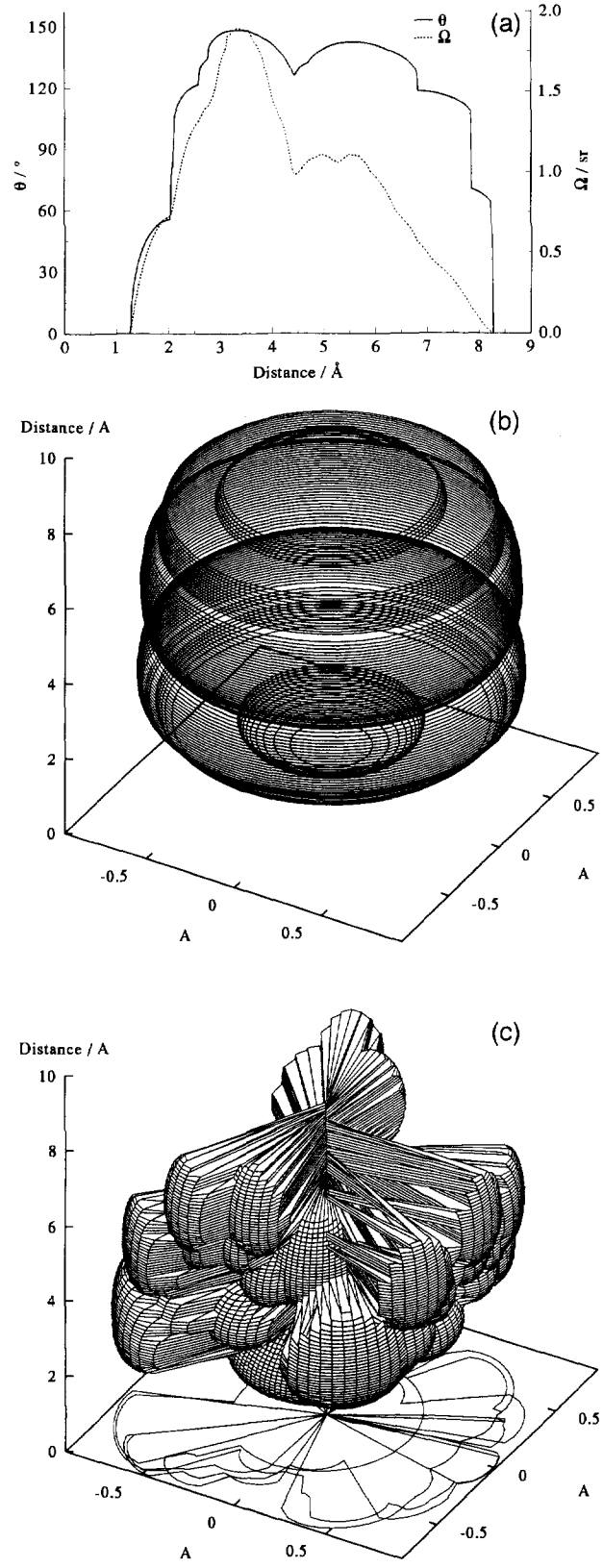

Fig. 9. (a) CARP for PPh_3. The measurements used to generate the figure are based on the Tolman cone angle methodology. (b) 3-D representation of a CARP for PPh_3. The measurements used to generate the figure are based on the Tolman cone angle methodology. (c) The variation of PPh_3 ligand profile (cone angle) with r_{CARP}.

Table 1
Covalent and van der Waals radii used in cone angle measurements

	Tolman [3]		Bondi [16]		Brown and coworkers [5]
	van der Waals/Å	Covalent/Å	van der Waals/Å	Covalent/Å	van der Waals/Å
H	1.00	0.33	1.20	0.37	1.42
C [a]	[1.60]	0.77	1.70	0.77	1.90
P	—	0.96	1.80	1.06	2.18
O	1.35	0.66	1.52	0.73	1.74

[a] sp^3 carbon atom.

CARPs it is possible to determine the significant point of interaction between two adjacent ligands, provided the angular meshing issue is neglected.

A similar analysis has been undertaken for ligand solid angles [16]. Quantification of the overlap for solid angles has been achieved [16] and this approach can also be used in principle for cone angles. Thus, CARPs can be used to provide a pictorial representation of the volume in space in which cone angles of ligands can overlap. A consideration of the CARPs for PH_3, PMe_3, PEt_3 and PPh_3 reveals that they all have θ_{max} at ca. 3 Å and all have a 'flat' maxima. This would suggest that if any of these ligands are attached to the same apex (metal) that the ligand–ligand interaction will be little influenced by the metal–phosphorus bond length. (This argument will of course not necessarily hold true for other ligands.) The steric constraint will be determined predominately by θ_{max}.

Comparison of the CARP and the angle radial profile (SARP) is also revealing in terms of the shapes of the curves generated by the two different ligand shape measurements. SARPs for PH_3, PMe_3, PEt_3 and PPh_3 are shown in Fig. 6(a), Fig. 7(a), Fig. 8(a) and Fig. 9(a) respectively.

For PH_3 (Fig. 6(a)) the major difference between the SARP and the CARP relates to the values at large distance measurements. In the cone angle method the ligand sizes are larger than determined using solid angles (see below). This is also seen in Fig. 7(a), Fig. 8(a) and Fig. 9(a). The position of θ_{max} and Ω_{max} need not be the same, as is shown e.g. for the PEt_3 data (Fig. 8(a)). Note that the units used for the different measures, θ and Ω, are different, and so a direct comparison in absolute terms is not possible.

3.3.1. Choice of atomic and covalent radii

The choice of van der Waals radii and covalent radii for use in cone angle calculations has been little discussed in the literature. The original choices made by Tolman were determined by the CPK model construction kits (Table 1), and these values have since been used extensively by other workers in the field. These radii do, however, differ from those given by Bondi [14] (Table 1) or modified by Gavezzotti [17]. Further, the values used by Brown and coworkers in E_R calculations [5] are also different (Table 1). A major difference between the Bondi and Tolman data relates to the choice of the van der Waals radius for hydrogen.

We have analysed the effect of variation of the van der Waals radii of hydrogen on the cone angle measurement for PH_3 to establish whether this is an important variable in steric measurements. The results are shown in Fig. 10. Two points are to be noted from the figure.

(i) The position of the cone angle maximum of L varies in a predictable manner for most of the data. This would suggest that provided consistency is applied in the choice of the atom radii then the choice of the van der Waals radii of a particular series of complexes is arbitrary.

(ii) The diagram does, however, indicate that if the radius for H is chosen to be too small then the position of the maximum cone angle of a PR_3 ligand will shift to the P atom ($r \sim 2.0$ Å; $r_H < 0.6$ Å). While this is not an issue for PH_3, the issue is significant for more complex ligands, and a change from 1.2 Å to 1.0 Å can result in variation in the position of θ_{max}.

3.4. Evaluation of θ for a constrained ligand

The measurement of CARPs for the constrained small ligand, $P(OCH_2)_3CCH_3$, in a range of different metal environments was chosen for study. This ligand should show little flexibility in its shape and provide a test of

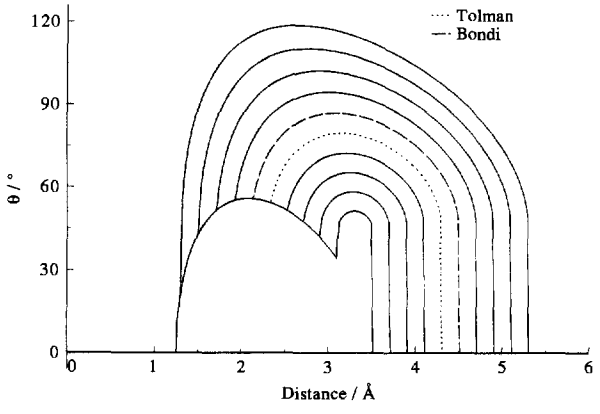

Fig. 10. CARP for PH_3 showing variation of θ_{max} with distance as a function of r_H.

the CARP methodology and indicate further the limitations of the original Tolman cone angle.

Table 2 contains a listing of known organometallic complexes containing $P(OCH_2)_3CCH_3$ whose crystal structures have been reported in the Cambridge Crystallographic Database. The data generated by molecular mechanics calculations (SYBYL) for the phosphite ligand in a $Cr(CO)_5$ environment are also included for completeness [5]. The table contains Tolman cone angles, measured with atomic radii used by Bondi [14], at two different M–P distances. In the first column the θ'_{max} recorded is the value measured using the actual crystallographic data; in the second column θ_{max} is the value measured with d_{M-P} set at 2.28 Å (Tolman distance). Consideration of θ_{max} suggests that the experimentally determined value is $59 \pm 1°$ with a slight variation in the position of the maxima (2.76–2.79 Å). This value is different from the energy minimized data [5] obtained for $Cr(CO)_5L$. Fig. 11 shows a CARP for the ligand in the different metal environments which highlights the regions in which the shape of the $P(OCH_2)_3CCH_3$ varies.

Of greater significance are the θ' measurements, i.e. the Tolman cone angles measured using the crystallographic data. Here we see much more scatter both in terms of the θ'_{max} value (56–62°, avg. $59 \pm 3°$) and the position of the θ'_{max} (1.82–2.94 Å). The value of θ'_{max} for CoL_5^+ needs comment. Here, we note that the value has actually shifted from the H atom on the CH_2 to the P atom (ca. 1 Å shift). (A consideration of Fig. 11 gives a pictorial representation of where the θ'_{max} for the CH_2 and P atoms would appear.)

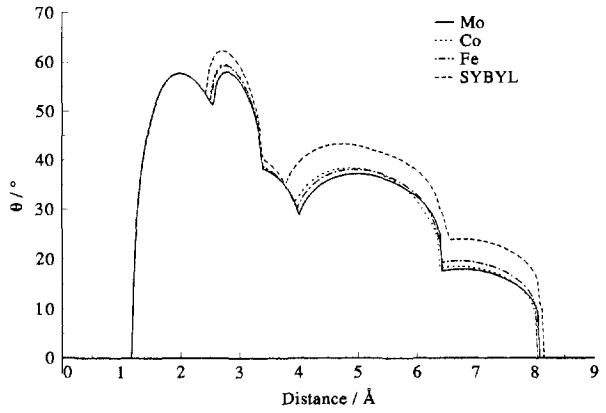

Fig. 11. CARP for four structures listed in Table 2 (Mo = $Mo(CO)_5L$, Co = $Co(\eta^5\text{-}C_5H_5)(I)_2L$; Fe = $Fe(CO)_2(CHF)L$; Cr = $Cr(CO)_5L$).

Calculations were also carried out using $r_H = 1.00$ Å (instead of 1.2 Å); in this instance the θ'_{max} moved to the P atom for more of the complexes.

The above analysis on a constrained ligand gives some indication of the difficulty that can be expected for assessment of the size of an unconstrained ligand using Tolman cone angles. Clearly θ_{max} values will be influenced by both the metal environment and the choice of covalent and van der Waals radii. Analysis of data for ligands with many possible conformers is under way and will be reported elsewhere.

Table 2
Cone angles for $P(OCH_2)_3CMe$

Complex [a]	θ'_{max} /deg [b]	θ_{max} /deg [c]
$Fe(CO)_2(CHF)L$ [d] [18]	62 (2.65)	59 (2.76)
$Co(\eta^5\text{-}C_5H_5)(I)_2L$ [19]	62 (2.63)	59 (2.76)
$Mo(CO)_5L$ [20]	56 (2.94)	58 (2.79)
$Cr(CO)_5L$ [e] [5]	61 (2.78)	62 (2.72)
$Os(CO)_3L_2Os(CO)_4W(CO)_5$ [21]		
CoL_5^+ [22]	60 (2.80)	60 (2.76) [f]
	62 (1.82) [g]	58 (2.78) [f]

[a] $L = P(OCH_2)_3CCH_3$. [b] Cone angle as measured from crystallographic data; distance (Å) of θ'_{max} from the metal given in brackets. [c] Cone angle as measured from the metal at the Tolman distance of 2.28 Å; distance (Å) of θ_{max} from the metal given in brackets. [d] $CHF = C_{15}H_7F_{12}$

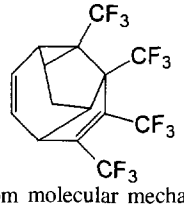

[e] Value determined from molecular mechanics calculations [13]. [f] Average of all the $P(OCH_2)_3CCH_3$ groups. [g] θ_{max} has moved to correspond to the position of the P atom.

4. Conclusion

A consideration of the assumptions used in deriving the Tolman cone angles has indicated a number of important issues which have not been discussed previously. A visual representation of a cone angle as determined at different positions along a metal–ligand bond axis reveals the angular symmetry implied in the calculation. This representation can readily be indicated by a CARP which indicates the θ_{max} as well as other features relating to the shape of the ligand. It is also clear that the meshing issue cannot be described by use of the original Tolman methodology. It is possible to represent the shape of the molecule, in a given conformer, in 3-D using a *ligand profile* measurement; however, to date it has not been possible to represent the change of θ with r_{CARP} adequately in a 2-D graph.

Quantification of the overlap between two adjacent ligands can be achieved by means of a number of procedures [16]. Qualitative analysis can be achieved by visual inspection of two or more ligand CARP diagrams. Thus, extension of the Tolman cone angle to a

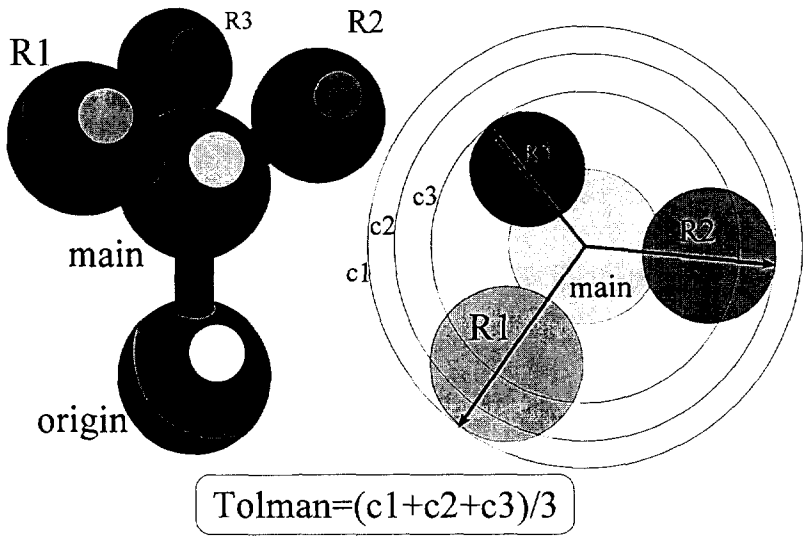

Fig. 12. Schematic diagram showing a 3-D representation of a typical ligand and a projected view along the metal–ligand bond.

third dimension provides a facile method of extending the original concept.

Acknowledgements

We wish to thank the FRD and the University for financial assistance. Helpful discussions with Dr. David White are gratefully acknowledged.

Appendix A. Calculation of the Tolman cone angle

The method used to calculate the Tolman cone angle in the computer algorithm involved two stages:

(1) the identification of the individual bonded groups to the central atom of the ligand;

(2) the calculation of the cone angle for each bonded group and the calculation of the average of these cone angles to give the Tolman cone angle.

The schematic diagram in Fig. 12 shows a 3-D representation of a typical ligand and a projected view down the metal ligand bond. The main atom is identified as the atom bonded to the metal atom, and the groups of interest are the molecular fragments bonded to this main atom. A common situation is to have three bonded groups, labelled R1, R2 and R3 in Fig. 12. Each of these groups may be composed of a number of bonded atoms, and may have a different size. This difference in angular size is clearly indicated in the schematic projection. For each group R1 to R3, all angles between the vector from the metal to the main atom and all the vectors from the metals to the individual atoms are calculated. The atom for which this angle plus the semi-vertex angle is a maximum is used for the calculation of the cone angle for that group, using the following equation:

$$\gamma_x = 2(\sigma_x + a_x)$$

Where γ_x is the cone angle for that group, a_x is the semi-vertex of the chosen atom, and the σ_x is the angle between the vector to the atom and the vector to the main atom.

Once the cone angles of all groups have been calculated, the Tolman cone angle is calculated as the average cone angle of the three groups. Normally the '×2' multiplication factor is done at the end, to optimize the calculation, resulting in the following final equation.

$$\gamma_{\text{Tolman}} = 2 \sum_{x=1}^{n} (\sigma_x + \alpha_x)$$

where γ_{Tolman} is the total Tolman cone angle and n is the number of groups bonded to the main atom.

It can be seen that if the bonded groups all have the same size, the Tolman cone angle represents a cone that bounds the entire ligand and has its origin at the metal atom.

References

[1] H. Schlenkluhn, W. Schiedt, B. Weimann and M. Zähres, *Angew. Chem. Int. Ed. Engl., 18* (1979) 401.

[2] M.N. Golovin, M.M. Rahman, J. Belmonte and W.P. Giering, *Organometallics, 4* (1985) 1981.

[3] C.A. Tolman, *Chem. Rev., 77* (1977) 33.

[4] (a) A. Immirzi and A. Musco, *Inorg. Chim. Acta, 25* (1977) L41. (b) D. White, B.C. Taverner, P.G.L. Leach and N.J. Coville, *J. Comput. Chem., 14* (1993) 1042. (c) M. Hirota, K. Sakakibara, T. Komatsuzaki and I. Akai, *Comput. Chem., 15* (1991) 241. (d) I. Akai, K. Sakakibara and M. Hirota, *Chem. Lett.*, (1992) 1317. (e) C.T. Komatsuzaki, I. Akai, K. Sakakibara

and M. Hirota, *Tetrahedron, 48* (1992) 1539. (f) R. Chauvin and H.B. Kagan, *Chirality, 3* (1991) 242. (g) P.B. Dias, M.E. Minas da Piedade and J.A.M. Simoes, *Coord. Chem. Rev., 135–136* (1994) 737.

[5] (a) M.L. Caffery and T.L. Brown, *Inorg. Chem., 30* (1991) 3907. (b) K.J. Lee and T.L. Brown, *Inorg. Chem., 31* (1992) 289. (c) T.L. Brown, *Inorg. Chem., 31* (1992) 1286.

[6] (a) D. White and N.J. Coville, *Adv. Organomet. Chem., 36* (1994) 95. (b) T.L. Brown and K.J. Lee, *Coord. Chem. Rev.*, 128 (1993) 89.

[7] A.L. Seligson and W.C. Trogler, *J. Am. Chem. Soc., 113* (1991) 2520.

[8] N.J. Coville, M.S. Loonat, D. White and L. Carlton, *Organometallics, 11* (1992) 1082.

[9] (a) Y. Yamamoto, K. Aoki and H. Yamazaki, *Inorg. Chem., 18* (1979) 1681. (b) P.P.M. de Lange, H.-W. Frühauf, M.J.A. Kraakman, M. van Wijnkoop, M. Kranenburg, A.H.J.P. Groot and K. Vrieze, *Organometallics, 12* (1993) 417.

[10] D. Datta and D. Majumdar, *J. Phys. Org. Chem., 4* (1991) 611.

[11] (a) G. Ferguson, P.J. Roberts, E.C. Alyea and M. Khan, *Inorg. Chem., 17* (1978) 2965. (b) D.H. Farrar and N.C. Payne, *Inorg. Chem., 20* (1981) 82. (c) E.C. Alyea, G. Ferguson and A. Somogyvani, *Inorg. Chem., 21* (1982) 1369.

[12] J.D. Smith and J.D. Oliver, *Inorg. Chem., 17* (1978) 2585.

[13] D. White, B.C. Taverner, P.G. Leach and N.J. Coville *J. Organomet. Chem., 478* (1994) 205.

[14] A. Bondi, *J. Phys. Chem., 68* (1964) 441.

[15] L. Stahl and R.D. Ernst, *J. Am. Chem. Soc., 109* (1987) 5673.

[16] D. White, C. Taverner, P.G. Leach and N.J. Coville, submitted.

[17] A. Gavezzotti, *J. Am. Chem. Soc., 105* (1983) 5220.

[18] R. Goddard and P. Woodward *J. Chem. Soc. Dalton Trans.*, (1979) 711.

[19] R.V. Davis and J.G. Verkade, *Inorg. Chem., 29* (1990) 4983.

[20] M.J. Aroney, M.S. Davies, T.W. Hambley and R.K. Pierens, *J. Chem. Soc. Dalton Trans.*, (1994) 91.

[21] R.J. Batchelor, H.B. Davis, F.W.B. Einstein and R.K. Pomeroy, *J. Am. Chem. Soc., 112* (1990) 2036.

[22] J.O. Albright, J.C. Clardy and J.G. Verkade, *Inorg. Chem., 16* (1977) 1575.